

scope

Contemporary Research Topics

work-based learning 4: Technology

November 2022

<https://doi.org/10.34074/scop.6004004>

DENOISING ACOUSTIC EMISSION SIGNAL USING

EMPIRICAL MODE DECOMPOSITION METHOD

Zazilah May, M. K. Alam, Nazrul Anuar Nayan, and S. A. Latif

Published by Otago Polytechnic Press. Otago Polytechnic Ltd is a subsidiary of
Te Pūkenga, New Zealand Institute of Skills and Technology.

© 2022 the authors; © illustrations, the artists or other copyright owners.

DENOISING ACOUSTIC EMISSION SIGNAL USING EMPIRICAL MODE DECOMPOSITION METHOD

Zazilah May, M. K. Alam, Nazrul Anuar Nayan, and S. A. Latif

ABSTRACT

Acoustic emission (AE) plays an important role in Structural Health Monitoring (SHM) applications by providing the early-stage damage assessment of composite materials. However, the collection of AE signals is challenging due to complex noise arising from the mechanical equipment, temperature, vibration, friction as well as external and internal environments of the structure. In order to overcome this challenge, even though many denoising methods have been introduced to acquire the denoised AE signals, there is still a lack of effectiveness in denoising without degrading the originality of the AE signals. Therefore, this paper adopts an efficient denoising method named Empirical Mode Decomposition (EMD) to remove most of the noises of the acquired AE signals by keeping its original properties. The adopted method is initially utilised on synthetic datasets which are randomly generated inducing various levels of Gaussian white noise. The obtained results are then compared to the original properties of the randomly generated clean dataset to evaluate the effectiveness of the EMD method. Experiments have been carried out to acquire the AE signals added with friction and vibration noises and then the EMD method is applied to them to eliminate the noises. The performance of the EMD method has been evaluated based on different performance metrics. Results show that the EMD method effectively removes most of the noises without disrupting original properties of the AE signals.

INTRODUCTION

Acoustic emission (AE) has recently received significant interest in the area of structural health monitoring, especially for corrosion and crack detection, damage, and leakage monitoring. Acoustic emission is a transitory elastic wave phenomena generated by the change of some outer conditions such as temperature, stress, and so on (Joseph & Giurgiutiu, 2020). Acoustic emission signals generate a variety of monitoring characteristics, including amplitude, rising time, energy, and hit count, that can be utilised to inspect existing micro-cracks in concrete. These parameters are also utilised for determining the location of the micro-crack. Due to the fact that the AE signal is produced by a variety of other causes, including temperature, friction, and vibration, the collected AE signal has weak characteristics and overlapping frequency bands when compared to the complex noise background (Kharrat et al., 2016). To enable online structural damage identification, it is important to obtain a clear AE signal from a damage source against a noise background. Thus, noise reduction of AE signals is necessary in SHM applications when assessing the welded structure's damage.

Numerous denoising techniques have been introduced and implemented in the literature as a pre-processing tool outside of the data collecting system (Liu et al., 2018; Khamedi et al., 2019; He et al., 2020; Ji et al., 2018). Fast Fourier Transform (FFT) is a widely used denoising algorithm that is typically included into commercial AE data collecting systems. The FFT converts a time-domain signal to a time-frequency domain signal in order to obtain the

signal's frequency information and suppress non-essential aspects. While FFT is an excellent method for denoising, it produces a signal with a poor resolution and is incapable of doing time and frequency domain analysis concurrently (Liu et al., 2018). Additionally, FFT is inefficient when dealing with non-stationary and transient inputs (Liu et al., 2018). In comparison, wavelet transform (WT) is another renowned denoising technique which is based on the linear transformation. In WT, the basic functions are modified by following the scaling function of a "mother wavelet" (Satour et al., 2014). Discrete Wavelet Transform (DWT) (Ramos et al., 2017), Wavelet Packet Transform (WPT) (Khamedi et al., 2019) and Stationary Wavelet Transform (SWT) (Nason & Silverman, 1995) are some of the most utilised denoising methods in the WT family that eliminate the various types of the noise of AE signal coming from the damage portions of the weld materials. The expanded DWT models such as WPT and SWT provide the details resolution for the AE signal. An eye-catching noise reduction has been gained for the non-stationary AE signals through its multi-resolution properties (He et al., 2020). However, the obtained AE signal is sensitive to the nature of the application, which may include random noise. Several sources of noise are typically added to the AE signals during collecting, including ambient and internal noise, mechanical equipment, vibration, friction, and white noise. These noises may serve as a misleading means of deriving required knowledge from the signals. Thus, these noises of the AE signal should be suppressed before performing the knowledge-discovery methods. We use the Empirical Mode Decomposition (EMD) approach in this research to decompose the AE signal into multiple components based on the signal's frequency information and magnitude. To achieve gain in denoising, unwanted components are removed using Euclidean distance calculations and then the transformed signal is reconstructed to provide the denoised AE signal.

The remainder of this article is structured as follows: The materials and methods section discusses the data acquisition system and the denoising method used, as well as many evaluation criteria. The following section analyses the results and discussions. The article ends with the conclusion.

MATERIALS AND METHODS

This section discusses different characteristics along with some parameters of the test specimens. The AE data acquisition system's experimental details are provided.

Acoustic emission signal acquisition

Continuous AE signals were recorded during the hydrogen evolution process. The signals were analysed using a four-channels data collection system equipped with an integrated low-noise preamplifier. In this study, a piezoelectric sensor with an acquisition threshold set to a specific decibel level was used. The sensors and coupling agent are attached to the specimen and fixed with a magnetic holder in a four-clock position (12, 3, 6, 9 o'clock) on a carbon-steel pipe. Physical Acoustics Corporation supplies the entire system, including the AE sensors (USA). Prior to the tensile test, the signal acquisition system was calibrated using the pencil lead break technique. Numerous acquisition software parameters, such as hit definition time (HDT), peak definition time (PDT), and hit lockout time (HLT), have been given in Table 1. Setting these values is dependent on the material's type and nature, positioning of the active region and the AE sensors. In our data collecting system, each AE strike generates 1024 discrete data points. AEwin software (Express-8 and version V5.92) manufactured by MISTRAS was used to capture AE signals.

PARAMETER	VALUE
Hit definition time (HDT)	2000 μ s
Peak definition time (PDT)	1000 μ s
Hit lockout value (HLT)	500 μ s
Threshold value	40 dB
Sample rate	1 μ s per sample

Table 1. Acoustic emission parameters.

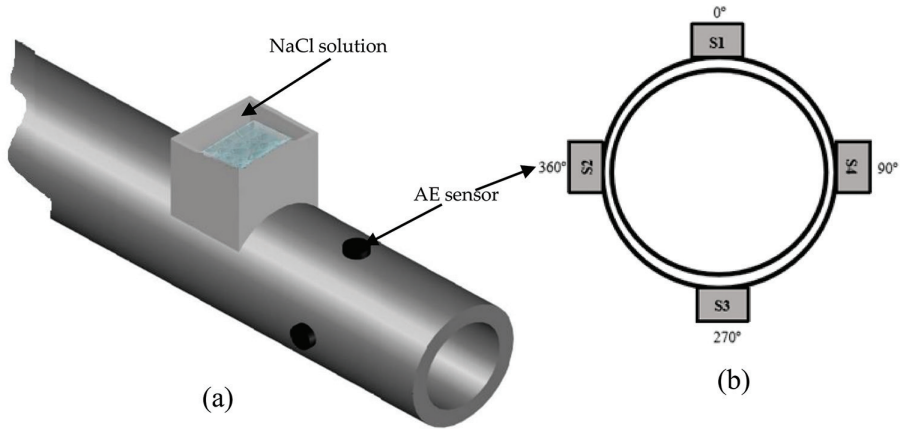


Figure 1. Schematic diagram for (a) cathodic hydrogen charging setup and (b) cross section pipe with location of sensors.

Denoising signal based on EMD

Huang (2014) created Empirical Mode Decomposition (EMD), an adaptive time-frequency decomposition method that makes use of the Hilbert–Huang Transform (HHT) for time-frequency analysis. The EMD method's primary characteristic is that it converts a given signal $x(t)$ into a total of oscillatory functions dubbed the Intrinsic Mode Function (IMF). The shifting process is carried out to obtain the IMF. The EMD technique requires that an IMF should satisfy two conditions: firstly, the sum of the maxima and minima, and the zero-crossing number must be 1; secondly, the local average must be 0. The signal is split into numerous IMFs based on its time scale properties. EMD decomposes the given original signal $x(t)$ as shown in Equation 1:

$$x(t) = \sum_{i=1}^n IMF_i(t) + rn(t) \quad (1)$$

where $IMF_i(t)$ and $rn(t)$ denote the IMF components' sequence and residual component, respectively. The first IMF shows an impact of high frequency, while the impact of subsequent IMFs declines proportionately until a non-smooth signal gained. By choosing the best IMFs which has residual components and high frequency, the signal may be reconstructed. The true IMFs are determined by determining the Euclidean distance, d , between the first IMF and the remaining IMF components, as shown in Equation 2.

$$d = \sqrt{\sum_{i=1}^n |x_i - y_i|^2} \quad (2)$$

where x_i and y_i are the i^{th} respective samples of the observed signal and the extracted IMF. The redundant IMFs have shape and frequency content different than those of the original signal. So, the value of d for redundant IMFs will be maximal. When IMFs are not appropriate, the value of d presents a maximum value.

The EMD method's efficacy in denoising signals is evaluated using a variety of performance indicators, including Signal-to-Noise Ratio (SNR), Root Mean Square Error (RMSE), and cross-correlation. The explanations with the mathematical equations are presented as follows:

SNR: It is a comparison between the levels of signal noise in original signal $x(l)$ and desired denoised signal $\bar{x}(l)$. SNR is the ratio of original mean signal power and mean noise power, and it is represented by the following equations.

$$SNR = 10 \log_{10} \left[\frac{\sum_{l=1}^n x^2(l)}{\sum_l [\bar{x}(l) - x(l)]^2} \right] \quad (3)$$

RMSE: It is applied to calculate the error of reconstruction generally after denoising a signal. This may be estimated by taking the root of the ratio between the total number of samples in the signal and the mean-square difference between the original signal $x(l)$ and the denoised signal $\bar{x}(l)$. The following definition applies to the RMSE:

$$RMSE = \sqrt{\frac{\sum_{l=1}^n [x(l) - \bar{x}(l)]^2}{n}} \quad (4)$$

Cross-Correlation ($xcorr$): It is used to determine the similarity between two discrete time sequences. If the cross-correlation value $xcorr$ is near to 1, the cleaned signal and the signal with noise have a high degree of similarity. The cross-correlation can be stated in the following way:

$$xcorr = \left[\frac{E(\bar{x}(n) - \mu_x)(x(n) - \mu_x)}{\delta_x - \delta_x} \right] \quad (5)$$

where $\mu_{\bar{x}}$ and μ_x represent the mean values of the denoised signal $\bar{x}(n)$ and the noisy signal $x(n)$, respectively, and $\delta_{\bar{x}}$ and δ_x signify the two signals' corresponding standard deviations. The statistical expectation or mean function is denoted by the operator $E()$.

RESULTS AND DISCUSSION

This section describes the simulation environment, datasets, and parameters used in the experimentation.

Simulation setup and datasets

Experimental AE data are gathered during hydrogen evolution and artificially generated friction and vibration noises on the carbon steel pipeline (May et al., 2020). Additionally, the synthetic datasets are created at random using varying degrees of Gaussian white noise. Following that, the adopted EMD approach is applied to both types of datasets to evaluate the denoising performance of our denoising method. In AE datasets, there is just one type of measurement (AE signal amplitude in mV), which is captured as waveforms at each microsecond sampling interval and consists of 1024 measurements. The EMD approach was applied to the first 1000 waveforms of a single AE sensor, resulting in a total of 1,024,000 discrete time points being measured. In comparison, the synthetic datasets are generated algorithmically and include signal-to-noise ratios (SNR) of 5 dB, 10 dB, 15 dB, 20 dB, and 25 dB. The datasets are one second in length and sampled at a rate of one millisecond. Additionally, simulations on the datasets are run in the MATLAB environment to evaluate the EMD denoising method's performance.

Denosing of synthetic datasets using Gaussian white noise in accordance with EMD

The algorithmically created sinusoidal clean signal is displayed in Figure 2, along with artificially inserted Gaussian white noise signals at various levels of SNR, including 5 dB, 10 dB, 15 dB, 20 dB, and 25 dB. The vertical axis of the graphic represents the signal's amplitude, while the horizontal axis represents time. The synthetic clean signal is utilised as a reference signal, and the EMD-based denoising approach is applied to randomly produced noisy signals to evaluate its performance in terms of denoising accuracy without affecting the reference signal's essential features. In Figure 3, we compare simulated clean signals to EMD-based denoised signals in order to measure the EMD method's efficacy in removing various amounts of Gaussian white noise. Additionally, the performance of the EMD approach in denoising severe level noisy signals is evaluated using three criteria (SNR, root mean square error, and cross-correlation) and the resulting results are compared to those of noisy signals. As illustrated in Figure 3, even if there is a modest effect on the amplitude of the de-noised signals only in the case of extremely noisy signals, the remaining attributes of the de-noised signals are nearly identical to those of the clean signal. Additionally, the SNR and cross-correlation values obtained for EMD-based de-noised signals are higher with a smaller reconstruction error than the values obtained for noisy signals. Table 2 compares the performance of the clean signal,

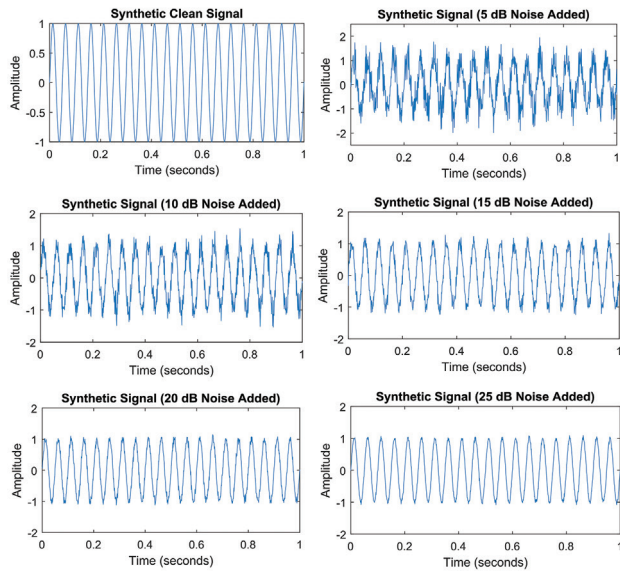


Figure 2. Synthetic clean signal and the signals with the addition of several degrees of Gaussian white noise.

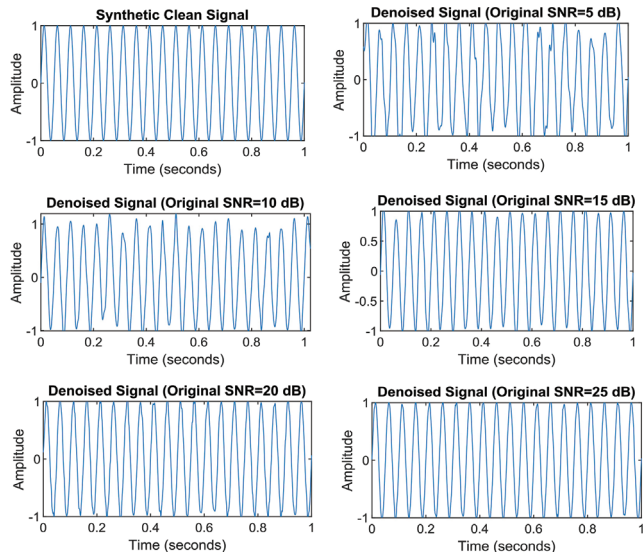


Figure 3. Comparison between synthetic clean signal and the EMD-based denoised signals.

the properties of various levels of noisy signals, and the properties of EMD-based de-noised signals. According to Table 2, all attributes of the clean signal except the “Max Peak Frequency” feature are altered by the various degrees of Gaussian white noise. However, the EMD denoising approach effectively removes multiple levels of noise, and the denoised signals have essentially identical qualities to the clean signal. Thus, it can be asserted that EMD is an effective method for denoising extremely noisy signals without impairing the signal’s core features.

Denoising of frictional noisy AE signal using EMD method

By rubbing a steel plate against the same test specimen and adjusting the other settings as indicated in the Materials and Methods section the frictional noisy AE signal was captured. Then, using the proposed EMD approach, frictional noise is removed from the recorded AE signal, and the noise reduction performance is evaluated. The frictional noisy AE signal, the EMD-based de-noised signal, and estimated noise are all depicted in Figure 4. The de-noised EMD signal demonstrates how the EMD approach effectively lowers frictional noise while retaining critical AE information.

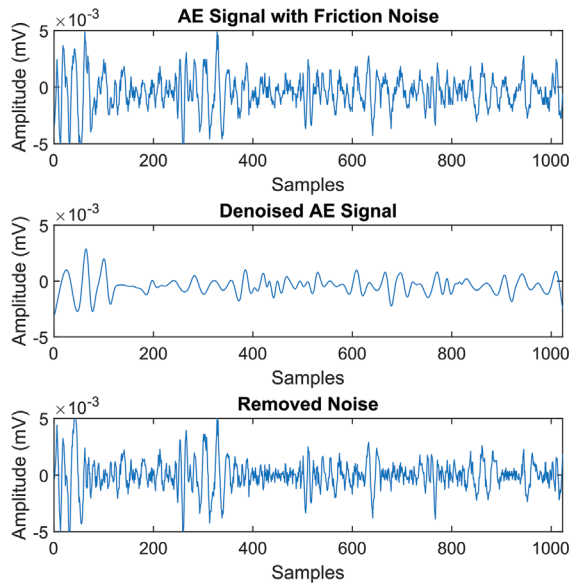


Figure 4. Comparison among frictional noisy AE signal, the AE signal after EMD-based denoising and estimated noise.

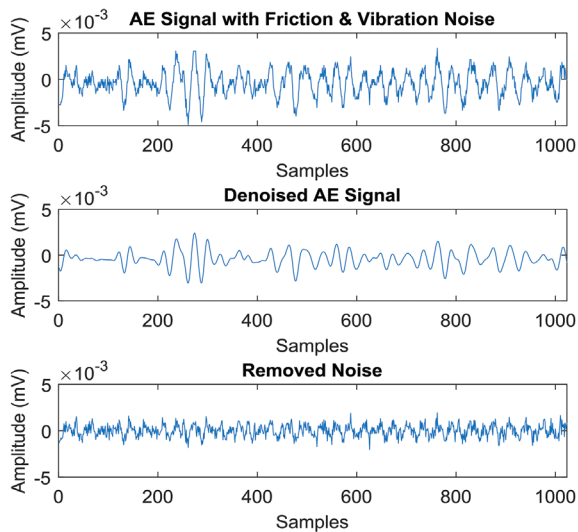


Figure 5. Comparison among frictional and vibrational noisy AE signal, the signal after EMD-based denoising and estimated noise.

Denoising of frictional and vibrational noisy AE signal using EMD method

As mentioned previously, frictional and vibrational noise were determined by rubbing and pounding on the same object during the experiment. To remove both noises from the collected noisy AE signal, the EMD denoising method is used and the denoising performance is compared to the original noisy AE signal. The frictional and vibrational noisy AE signals, the EMD-based de-noised signal, and predicted noise are all shown in Figure 5. The de-noised EMD signal in Figure 5 demonstrates that the EMD approach effectively eliminates both noise and critical AE information. Thus, the EMD denoising method can be used to decrease not only frictional noise, but also vibrational noise in AE data obtained from SHM applications.

Properties	Clean Signal	25 dB	20 dB	15 dB	10 dB	5 dB
Number of Peaks	21.00	209.00	209.00	209.00	273.00	338.00
Max Peak Frequency (Hz)	19.53	19.53	19.53	19.53	19.53	19.53
Mean Frequency (Hz)	19.80	20.53	22.01	26.58	41.27	71.47
Angular Frequency (Hz)	125.54	1291.41	1291.41	1690.43	1970.83	2082.04
RMS Bandwidth (kHz)	0.87	60.24	60.24	110.20	107.47	101.97
Mean Frequency Power (dB)	-6.01	-5.97	-5.86	-5.80	-5.30	-4.26
RMSE	0.00	0.04	0.07	0.12	0.23	0.38
SNR (dBc)		24.49	20.91	15.66	9.29	6.04
xcorr (%)	100.00	99.84	99.52	98.48	95.17	87.76
EMD-Based denoised signals						
Number of Peaks	21.00	21.00	21.00	21.00	22.00	29.00
Max Peak Frequency (Hz)	19.53	19.53	19.53	19.53	19.53	19.53
Mean Frequency (Hz)	19.80	19.88	20.01	19.94	20.02	20.39
Angular Frequency (Hz)	125.54	125.92	132.21	125.79	131.82	176.11
RMS Bandwidth (kHz)	0.87	0.87	0.84	0.84	0.86	1.53
Mean Power (dB)	-6.01	-5.96	-6.12	-6.19	-6.01	-5.21
RMSE	0.00	0.03	0.04	0.06	0.10	0.17
SNR (dB)		32.54	26.52	23.06	19.76	16.98
xcorr (%)	100.00	99.94	99.82	99.68	99.09	97.34

Table 2. Comparison among the properties of synthetic clean signal, different degrees of noisy signals and the EMD-based denoised signals.

Hilbert frequency spectrum of the noisy AE signals and EMD-based denoised signals

According to Wu et al. (2015), the usual frequency spectrum of the generated AE signal is focused between 20 and 80 kHz during hydrogen evolution activity. This frequency range is mostly determined by bubble formation during hydrogen evolution activity and the level of induced potential. The Hilbert frequency spectrum of the original frictional and vibrational noisy AE signals is compared to the frequency spectrum of the de-noised AE signals generated using EMD in Figure 6. As seen in the plot, the frictional and vibrational noisy signals produce primarily overlapping frequency bands and have a negligible effect on the magnitude. The EMD method eliminates superfluous frequency components while retaining the useful frequency spectrum, as seen in Figure 6 by the EMD-based denoised Hilbert spectrum.

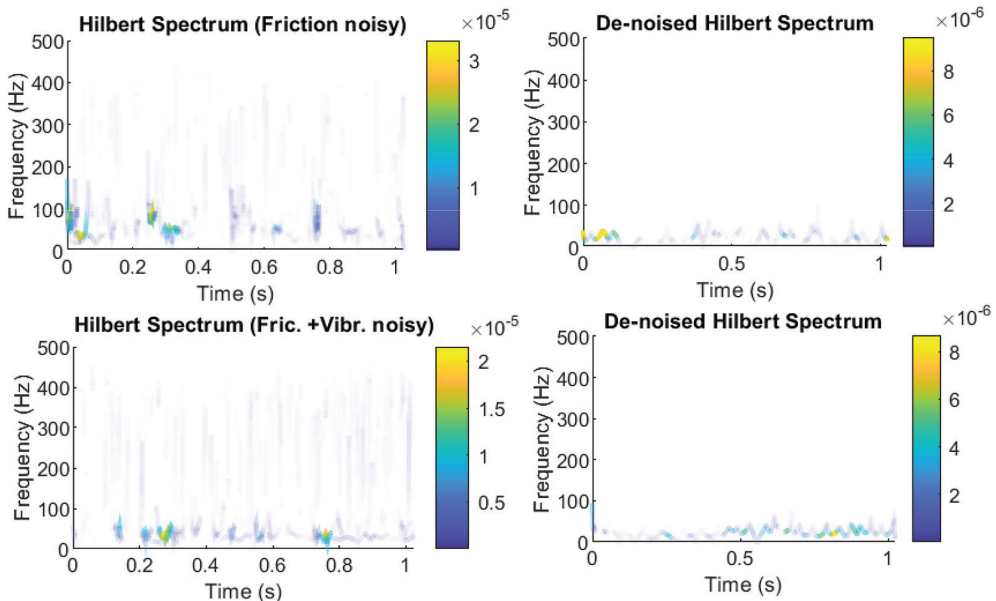


Figure. 6. Comparison among Hilbert spectrum of the Original noisy AE signals and EMD-based denoised AE signals.

CONCLUSION

According to the findings and analyses of this work, the denoising method is critical in a variety of applications in SHM for the gathering of cleaned AE signals to increase the effectiveness of early-stage damage assessments. By minimising the reconstruction error, the adopted EMD approach significantly reduces the noise in AE signals gathered during tests, making it effective for extremely noisy AE signals recovered from a variety of monitoring applications in SHM. The simulation results produced using the EMD method demonstrate that the properties of the EMD-based de-noised signal are nearly identical to those of the original clean signal. Additionally, the outcomes of evaluation criteria such as SNR, RMSE, and cross-correlation are improved when using de-noised signals as opposed to noisy signals. The EMD denoising technique may be used to effectively capture AE clean signals during SHM inspection in real-world situations. However, preparatory study should be undertaken to determine the acquisition parameters based on the wavelength, threshold value, the accuracy of the AE sensor, and the wave velocity for a particular structure. Appropriate parameter selection can aid in the removal of reflected waves and other unwanted noise. This study can be expanded to include real-world SHM applications for the gathering of cleaned AE signals to evaluate the EMD method's denoising performance.

ACKNOWLEDGMENTS

The authors would like to express their gratitude to YUTP-FRG 2020 (Grant number 015LCO-187) for providing financial assistance for this research through research grants.

Zazilah May received her Bachelor's degree in Mathematics from University of Leicester, United Kingdom, in 1998, and the Master's degree in Advanced Control from UMIST, United Kingdom, in 2000. Currently, she is working as lecturer in the Electrical & Electronic Engineering Department, Universiti Teknologi PETRONAS (UTP), Malaysia. She has more than 20 years of professional experience in teaching and research in Malaysia. Her research interests lie in wireless communication, control systems, artificial intelligence, signal processing and image processing. She is involved in various projects related to oil & gas structural health monitoring.

M. K. Alam received his Ph.D. in Electrical and Electronic Engineering at Universiti Teknologi PETRONAS (UTP) in Malaysia. His research interest is in the field of Information Technology (Machine learning, Time-series data analysis, Time-series prediction, Data clustering, Data aggregation, Data compression).

Nazrul Anuar Nayan is a senior lecturer and researcher at the Department of Electrical, Electronic and Systems Engineering, Faculty of Engineering & Built Environment, Universiti Kebangsaan Malaysia (UKM), Bangi Selangor. He teaches in the area of biomedical signal processing and microelectronics.

Suhaimi Abd-Latif (Hymie Abd-Latif) is a Principal Lecturer at the College of Work Based Learning, Otago Polytechnic – Te Pūkenga, Aotearoa New Zealand. He is a Facilitator and Assessor for the Bachelor of Engineering Technology and New Zealand Diploma of Construction (Construction Management) in the Independent Learning Pathway (ILP) Programme.

 <https://orcid.org/0000-0002-0941-7721>

REFERENCES

- He, K., Xia, Z., Si, Y., Lu, Q., & Peng, Y. (2020). Noise reduction of welding crack AE signal based on EMD and wavelet packet. *Sensors*, 20(3), 761.
- Huang, N. E. (2014). Introduction to the Hilbert–Huang transform and its related mathematical problems. In N. E. Huang & S. S. P. Shen (Eds.), *Hilbert–Huang transform and its applications* (pp. 1–26). World Scientific.
- Ji, J., Li, Y., Liu, C., Wang, D., & Jing, H. (2018). Application of EMD technology in leakage acoustic characteristic extraction of gas-liquid, two-phase flow pipelines. *Shock and Vibration*, 2018.
- Joseph, R. & Giurgiutiu, V. (2020). Analytical and experimental study of fatigue-crack-growth AE signals in thin sheet metals. *Sensors*, 20(20), 5835.
- Khamedi, R., Abdi, S., Ghorbani, A., Ghiami, A., & Erden, S. (2019). Damage characterization of carbon/epoxy composites using acoustic emission signals wavelet analysis. *Composite Interfaces*.
- Kharrat, M., Ramasso, E., Placet, V., & Boubakar, M. (2016). A signal processing approach for enhanced acoustic emission data analysis in high activity systems: Application to organic matrix composites. *Mechanical Systems and Signal Processing*, 70, 1038–1055.
- Liu, X.-L., Liu, Z., Li, X.-B., Rao, M., & Dong, L.-J. (2018). Wavelet threshold de-noising of rock acoustic emission signals subjected to dynamic loads. *Journal of Geophysics and Engineering*, 15(4), 1160–1170.
- May, Z., Alam, M. K., Rahman, N. A., Mahmud, M. S., & Nayan, N. A. (2020, November 15). Denoising of hydrogen evolution acoustic emission signal based on non-decimated stationary wavelet transform. *Processes*, 8(11), 1460.
- Nason, G. P., & Silverman, B. W. (1995). The stationary wavelet transform and some statistical applications. In A. Antoniadis & G. Oppenheim (Eds.), *Wavelets and statistics* (pp. 281–299). Springer.
- Ramos, R., Valdez-Salas, B., Zlatev, R., Schorr-Wiener, M., & Bastidas Rull, J. M. (2017). The discrete wavelet transform and its application for noise removal in localized corrosion measurements. *International Journal of Corrosion*, 2017.
- Satour, A., Montrésor, S., Bentahar, M., Elguerjouma, R., & Boubenider, F. (2014). Acoustic emission signal denoising to improve damage analysis in glass fibre-reinforced composites. *Nondestructive Testing and Evaluation*, 29(1), 65–79.
- Wu, K., Jung, W.-S., & Byeon, J.-W. (2015). Acoustic emission of hydrogen bubbles on the counter electrode during pitting corrosion of 304 stainless steel. *Materials Transactions*, 56(4), 587–592.